CrossMark

Influence of oxidation state of phosphorus on the thermal and flammability of polyurea and epoxy resin

Thirumal Mariappan [a], Zhou You [b], Jianwei Hao [b], Charles A. Wilkie [a,*]

[a] Department of Chemistry and Fire Retardant Research Facility, Marquette University, PO Box 1881, Milwaukee, WI 53201, USA
[b] School of Material Science and Engineering, Beijing Institute of Technology, Beijing 100081, PR China

ARTICLE INFO

ABSTRACT

The focus of this study is an investigation of the effect of oxidation state of phosphorus in phosphorus-based flame retardants on the thermal and flame retardant properties of polyurea and epoxy resin. Three different oxidation states of phosphorus (phosphite, phosphate and phosphine oxide) additives, with different thermal stabilities at a constant phosphorus content (1.5 wt.%) have been utilized. Thermal and flame retardant properties were studied by TGA and cone calorimetry, respectively. The thermal stability of both polymers decreases upon the incorporation of phosphorus flame retardants irrespective of oxidation state and a greater amount of residue was observed in the case of phosphite. Phosphate was found to be better flame retardant in polyurea, whereas phosphite is suitable for epoxy resin. Phosphite will react with epoxy resin by trans-esterification, which is demonstrated by FTIR and ^{31}P NMR. Further, TG–FTIR and XPS studies also provide information on flame retardancy of both polymers with phosphorus flame retardants.

1. Introduction

Phosphorus-based flame retardants are widely used as effective flame retardants in the form of either additives or reactives and are particularly effective in oxygen containing polymers [1–4]. There are several forms of phosphorus-based flame retardants, both organic and inorganic, and these are available in various oxidation states, including phosphines (−3), phosphine oxides (−1), elemental phosphorus (0), phosphinates (+1), phosphites (+3), phosphonates (+3), phosphates (+5), etc. In addition, several synergistic combinations are known, including, phosphorus–halogen, phosphorus–nitrogen, phosphorus-intumescent, phosphorus–sulfur and phosphorus-inorganic nano-dimensional materials [5]. Due to environmental concerns emanating from halogen-based flame retardants, more attention has been paid recently to phosphorus-based retardants. Generally, phosphorus-containing flame retardants can act either in the gas phase, by flame inhibition, or in the condensed phase, to change the degradation pathway to one in which more char is produced and, necessarily, less volatiles. In both cases, the amount of heat released during combustion is reduced by the addition of the flame retardants [6,7].

Two reports describe the effect of oxidation state of phosphorus on the properties of carbon fiber reinforced epoxy composites and rigid polyurethane foam (PUF). Braun et al. have compared the thermal and fire retardant properties of carbon fiber reinforced epoxy with phosphine oxide, phosphinate, phosphonate and phosphate at 2.6 wt.% phosphorus content in the form of organophosphorus based curing agent. They found that the higher oxidation state of phosphorus showed poorer flame retardant properties than the lower oxidation state and with an increase in the oxidation state of phosphorus, the amount of char formation increases [8]. Lorenzetti et al. have used a constant (1.2 wt.%) phosphorus content of commercially available flame retardants (aluminum phosphinate, dimethyl propane phosphonate, triethylphosphate and ammonium polyphosphate) and studied the thermal behavior in rigid PUF. There is no interaction between

* Corresponding author. Tel.: +1 414 288 7239; fax: +1 414 288 7066.
E-mail address: charles.wilkie@marquette.edu (C.A. Wilkie).

PUF and the flame retardants, irrespective of oxidation state; the higher oxidation state flame retardants showed only condensed phase action compared to lower oxidation state of phosphorus flame retardant, which function in both the condensed and vapor phases [9]. Unfortunately, in neither report was phosphite considered.

Triphenylphosphate is a classic example of a gas phase fire retardant and has been investigated by Hastie [10]. The Schartel group has compared triphenylphosphate with larger arylphosphates and found that there is more condensed phase action when the decomposition temperature increases [11,12].

In this paper, three different oxidation states of phosphorus, triphenylphosphite (+3), triphenylphosphate (+5), and triphenylphosphine oxide (−1), all with similar substituents, are studied in both polyurea and epoxy resin at 1.5 wt.% phosphorus using commercially available flame retardants.

2. Experimental

2.1. Materials

The components for polyurea preparation involve part A, diisocyanate (polycarbodiimide modified diphenylmethane diisocyanate/Isonate 143L, Dow Chemical Company) and part B, diamine (poly(tetramethyleneoxide-di-p-aminobenzoate)/Versalink P1000, Air Products). These are mixed in the stoichiometric equivalent ratio of 1:4 w/w. The epoxy resin was based on the diglycidyl ether of bisphenol-A (Araldite GY6010) and aliphatic polyether amine (Jeffamine T403) as curing agents; both are obtained from Huntsman Advanced Materials. Triphenylphosphite (Doverphos 10, P content 10%), triphenylphosphate (Reofos TPP, P content 9.5%) and triphenylphosphine oxide (P content 10%) were used as flame retardants and were received from Dover Chemicals, Chemtura and Sigma Aldrich, respectively. Benzyl dimethyl amine (BDMA), CDCl$_3$ and 86% phosphoric acid were obtained from Sigma Aldrich as reagent grade. All chemicals were used as received.

2.2. Preparation of sample

The flame retardant polyurea and epoxy resin were prepared by a two-step method. At first the calculated quantity of diamine or epoxy oligomer and flame retardants (1.5 wt.% phosphorus content) were homogenously mixed with a mechanical stirrer and then the stoichiometric amount of curatives (diisocyanate for polyurea and diamine for epoxy) was added. Finally, the resultant mixture was poured into the aluminum mold, allowed to cure at room temperature for 12 h and then post cured (70 °C/24 h for polyurea, and 80 °C/2 h, 125 °C/3 h for epoxy resin). DSC analysis confirms the complete curing (disappearance of peak exotherm) of both polymers filled with phosphorus-based flame retardants.

2.3. Measurements

Fourier transform infrared (FTIR) spectra were performed on a Bruker TENSOR 27 spectrophotometer from 4000 to 600 cm^{-1} using ATR mode. ^{31}P NMR spectra were obtained using 10–25% solutions in deuterochlorform (CDCl$_3$) on a Varian 400 NMR (400 MHz) spectrometer. The phosphorus chemical shifts are relative to an external 86% aqueous phosphoric acid solution as reference.

The thermal stability of sample was measured on a SDT Q600, (TA Instruments) under a nitrogen (gas flow of 100 mL/min) atmosphere at a scan rate of 20 °C/min over a temperature range of 50–800 °C. Typical sample weights of 5–10 mg were employed. All samples were run at least in duplicate; temperature is reproducible to about ± 2 °C and mass to 0.2%.

The TGA–FTIR analysis was performed using a Netzsch TG 209 F1 Iris coupled to a Bruker Tensor 27 FTIR to study the thermal decomposition of the flame retarded samples. The analyses were conducted under a nitrogen atmosphere (flow rate 20 mL/min) at a heating rate of 20 °C/min over a temperature range of 30–700 °C. The sample weight was around 5 mg. The coupling system between the TG and FTIR was maintained at 200 °C to prevent condensation of the evolved gases.

The flame retardant properties were measured using a cone calorimeter (Atlas Cone 2) according to ASTM E1352 at a heat flux of 50 kW/m^2. The specimens for the cone calorimetric analysis were 100 mm × 100 mm × 6 mm (length × width × thickness) and three specimens per sample were measured and average values are reported. The results from cone calorimeter are generally considered to be reproducible to ±10%.

The elemental composition of the decomposed residue was analyzed using X-ray photoelectron spectroscopy (XPS), carried out on a PHI Quantera-II SXM (Ulvac-PHI, Inc.) using Al Kα radiation and an X-ray power of 2.5 kW under a vacuum of 2.6×10^{-7} Pa. The pass energy is 280 eV and the step length is 1 eV with a takeoff angle at 45°.

3. Results and discussion

The rapid linear polycondensation (without removal of by-products) of elastomeric polyurea (PU) without external catalyst and the ring opening condensation polymerization (without removal of by-products) of amine cured epoxy resin (EP) formation (a) and the chemical structure of different oxidation state of commercially available phosphorus flame retardants include triphenylphosphite [TPP$_i$, (b)], triphenylphosphate [TPP$_a$, (c)] and triphenylphosphine oxide [TPPO, (d)] are shown in Fig. 1. In the case of PU, the molecular chains are physically cross-linked microphase separated block copolymers of dispersed short oligomeric MDI hard segments aggregated through hydrogen bonds in the continuous long amorphous matrix of flexible (soft) segments, made of the high molecular weight diamine, that give extensibility to the PU. Interactions between chains, mainly hydrogen bonds between hard segments acting as a reinforcing filler, contribute to the properties of PU [13]. For EP, the hard and three-dimensional network structure is formed after chemical (amine) crosslinking at elevated temperature.
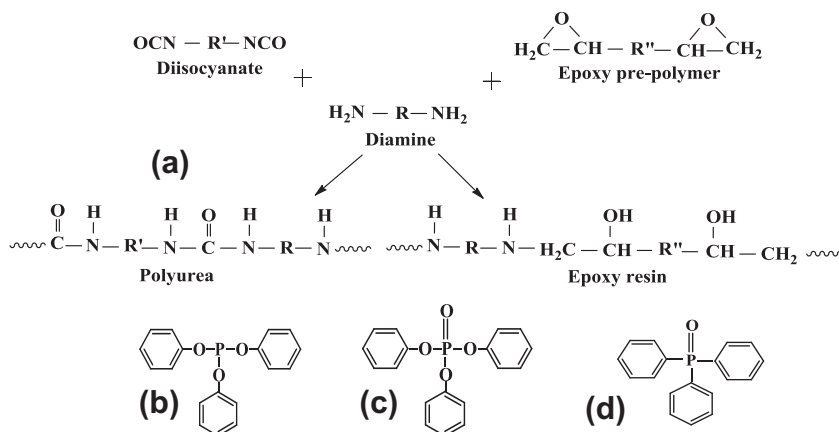
Fig. 1. Chemical structure of compounds: (a) preparation of polyurea and epoxy resin; (b) triphenylphosphite (TPP$_i$); (c) triphenylphosphate (TPP$_a$); (d) triphenylphosphine oxide (TPPO).

3.1. Thermal analysis

The thermal stability of flame retardants is important for processing, thermal stability, flame retardant properties and the end use polymer product applications. Fig. 2 shows the TG/DTG profiles of phosphorus flame retardants under inert conditions, i.e., in nitrogen. Although the amount of phosphorus present in the flame retardants is almost equal, TPPO showed slightly higher thermal stability ($T_{5\%}$ = 272 °C) compared to TPP$_a$ ($T_{5\%}$ = 242 °C) and TPP$_i$ ($T_{5\%}$ = 211 °C). This is likely due to the absence of the thermally weak link (C—O—P) in TPPO. All three phosphorus flame retardants display a single, rapid degradation with high T_{max} (maximum degradation temperature) values for TPPO (358 °C) than TPP$_a$ (313 °C) and TPP$_i$ (292 °C). All three flame retardants are completely volatilized at particularly 300, 325 and 365 °C for TPP$_i$, TPP$_a$ and TPPO, respectively.

Fig. 3 shows the TG/DTG profile of both PU and EP filled with different oxidation state phosphorus flame retardant additives. Neat PU shows a two step degradation processes while rapid single step decomposition takes place at about 400 °C in EP under a nitrogen atmosphere. The first and second degradation steps of PU take place in the temperature ranges 250–380 °C and 380–580 °C and the corresponding weight losses are 20 and 72 wt.%, respectively. The first step of degradation is mainly due to the degradation of the hard or urea segment because of its relatively low thermal stability. The second step can be attributed to the degradation of the soft segment [14]. The mass losses in the first and second degradations are in good agreement with the initial stoichiometry of the reactants. At higher temperatures, a small amount of residue (~7%) is retained in both polymers. Irrespective of the oxidation state of phosphorus, the thermal stability of both polymers decreases with the addition of phosphorus flame retardants. Moreover, the triphenylphosphite filled samples show poorer thermal stability than TPP$_a$ and TPPO. This may be due to the lower thermal stability of TPP$_i$ compared to the pristine polymers ($T_{5\%}$ = 319 °C for PU and EP, 372 °C). Both TPP$_a$ and TPPO provide almost the same thermal stability (onset and T_{max}) in PU, whereas in EP, nearly identical T_{max} values for both TPP$_i$ and TPP$_a$ are observed. There is no change in T_{max} of both polymers filled with TPPO. Despite the lower thermal stability of TPP$_i$, it shows a greater amount of residue in both polymers at high temperature compared to the other flame retardants which implies an interaction between the degradation products of the polymer with TPP$_i$ during pyrolysis. Compared to the pristine polymer, there is not much residue observed in the TPPO filled system, indicating that TPPO acts in the vapor phase and there are no chemical reactions occurring between degrading polymer and the additive.

3.2. Cone calorimetric analysis

Cone calorimetry is used to evaluate the fire retardant properties of both PU and EP; this technique is frequently considered to be the best indicator of performance in a full-scale fire. This provides information on the heat release rate (HRR) and especially its maximum value (PHRR); ignition time (t_{ign}); total heat released (THR); average mass loss rate (AMLR) and average specific extinction area (ASEA), a measure of smoke. Fig. 4 shows the heat release

Fig. 2. TG/DTG of phosphorus flame retardants.
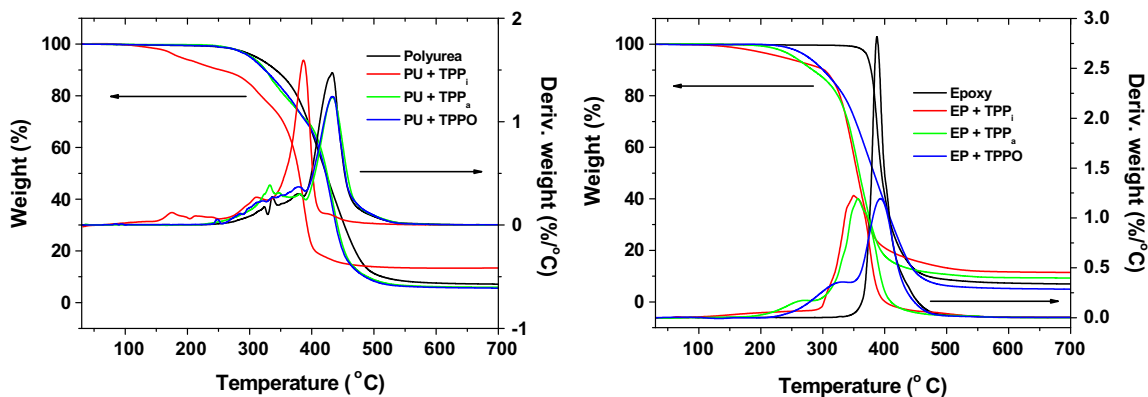
Fig. 3. TG/DTG of PU and EP filled different phosphorus compounds.
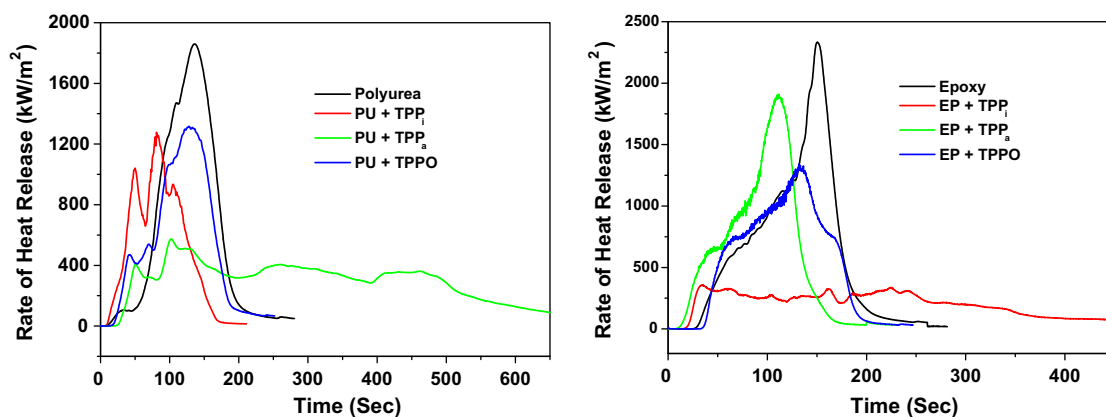
Fig. 4. Heat release curves of PU and EP filled with phosphorus compounds.

rate (HRR) curves of control and flame retarded PU and EP filled with different phosphorus flame retardant additives and the corresponding cone data are presented in Table 1. Both flame retarded samples showed prior and lower HRR compared to the controls. The earlier HRR of flame retarded samples is due to the lower thermal stability of the flame retardants. The HRR of PU is significantly decreased upon addition of TPP$_a$ but, for EP, the change occurs for TPP$_i$. It is likely that the formation of a large amount of char residue (intumescent) during burning, as shown in Fig. 5f, accounts for the greater flame resistance of EP [15]. Both TPP$_a$/PU and TPP$_i$/EP samples show lower HRR with prolonged burning behavior as compared to the other flame retardants and the control sample. The TPPO containing samples show the almost same time to peak HRR as samples filled with other flame retardants.

The time to ignition of PU increases with the addition of TPP$_a$ and TPPO, whereas higher ignition time is observed with TPPO filled EP. The higher ignition time of filled samples is due the gas phase action of the flame retardants. TPP$_i$ displays greater reduction of peak HRR of EP compared to other flame retardants, but the lower flame resistance of PU was observed with the addition of TPP$_i$. Likely the liquid TPP$_i$ plasticizes the PU matrix or hinders the PU formation reaction (cracks on the surface of the sample)

and thus decreases the cross-link density of PU. Also, there is no interaction between TPP$_i$ and PU during combustion so less char formation occurs during combustion, as shown in Fig. 5b. In addition, at room temperature (25 °C) in the absence of sun light, the surface of the TPP$_i$ filled PU sample undergoes a color change within one month, indicating that the physically blended liquid TPP$_i$ may possibly migrate towards the surface of the sample. TPP$_a$ shows better flame resistance and lower AMLR with PU compared to EP. All filled samples show low THR and higher smoke evolution compared to the control sample.

It is well known that TPP$_i$ act as a reactive diluent and Barnstorff et al. demonstrated that TPPi enters a polyamine cured EP through a trans-esterification reaction between the phosphite ester and the hydroxyl group present in the EP to form alkyl phenylphosphite derivatives, as shown in Fig. 6. It is apparent that the formation of the trans-esterification products (mono-, di- and tri alkyl phenyl phosphite) depends on the amount of free hydroxyl group [16].

The reaction between TPP$_i$ and hydroxyl group in the resin is examined through the measurement of gel time, FTIR and ^{31}P NMR spectroscopy. Table 2 shows the gel time of EP as it reacts with TPP$_i$, amine curing agent (Jeffamine T403) and the catalytically accelerated system. At constant

Table 1
Cone calorimetric data for PU and EP filled with phosphorus compounds.

Sample	t_{ign} (s)	P_{HRR} (kW/m^2) (% reduction)	THR (MJ/m^2)	AMLR (g/m^2 s)	ASEA (m^2/kg)
Polyurea	12 ± 4	1854 ± 65	160 ± 7	44 ± 5	452 ± 18
PU + 15% TPP$_i$	7 ± 1	1255 ± 63 (32)	116 ± 19	29 ± 11	525 ± 36
PU + 15% TPP$_a$	18 ± 3	637 ± 149 (66)	169 ± 23	15 ± 1	632 ± 11
PU + 15% TPPO	16 ± 1	1324 ± 23 (29)	130 ± 9	24 ± 3	999 ± 31
Epoxy resin	29 ± 3	2467 ± 150	164 ± 9	47 ± 2	753 ± 34
EP + 15% TPP$_i$	21 ± 1	504 ± 128 (80)	114 ± 5	18 ± 9	783 ± 163
EP + 15% TPP$_a$	12 ± 2	1959 ± 101 (21)	128 ± 1	52 ± 1	971 ± 111
EP + 15% TPPO	34 ± 1	1310 ± 63 (47)	126 ± 2	40 ± 5	845 ± 85

t_{ign}, Time to ignition; P_{HRR}, peak heat release rate; THR, total heat released; AMLR, average mass loss rate; ASEA, average specific extinction area, a measure of smoke.
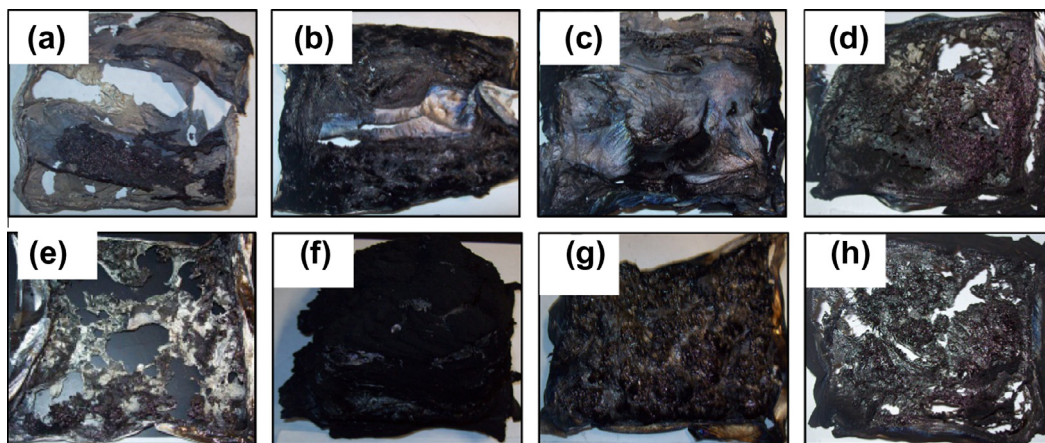
Fig. 5. Char images of flame retarded PU and EP after cone: (a) PU; (b) PU + TPP$_i$; (c) PU + TPP$_a$; (d) PU + TPPO; (e) EP; (f) EP + TPP$_i$; (g) EP + TPP$_a$; (h) EP + TPPO.
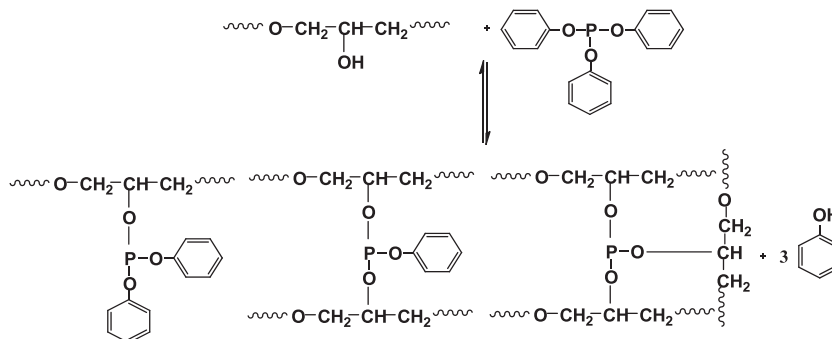
Fig. 6. The chemical interaction of epoxy resin with triphenyl phosphite.

temperature, the gel time decreases with the addition of TPP$_i$ (4 h) compared to the same amount of EP and curing agent (5 h) mixture. In the presence of BDMA, the gel time decreases for the TPP$_i$/EP mixture (54 h), whereas a prolonged gel time (72 h) and completely tack-free solid was observed after 92 h without amine curing agent, which implies that TPP$_i$ accelerates the curing reaction and is also involved in the cross-linking reaction to give a three-dimensional rigid network structure. As gel time increases the viscosity of resin mixture increases because of chain extension reactions. There is no change in viscosity of the

reaction mixture containing diamine with TPP$_i$, TPP$_a$ and TPPO. A similar observation is also noted for the EP containing TPP$_a$ and TPPO (also confirmed with FTIR, not shown here), which indicates that all phosphorus flame retardants are physically blended into both PU and EP, except TPP$_i$ with epoxy resin. TPP$_i$ is slowly oxidized to triphenylphosphate at RT, 59% conversion within 32 h [17]. To avoid this conversion, 0.1% of benzyl dimethyl amine (BDMA) accelerator was incorporated into TPP$_i$ containing EP and curing agent. The accelerated system shows 2 h gelation time at RT.

Table 2
^{31}P NMR chemical shifts (relative to 86% H_3PO_4, $\delta = 1.97$ ppm) of phosphorus compounds and their reaction with diamine and epoxy oligomer.

Sample	Chemical shifts (ppm)	Gel time (h)
TPP_i	126.1	–
TPP_a	−14.6	–
TPPO	33.1	–
Diamine + TPP_i	126.0, −14.6	–
Diamine + TPP_a	−14.6	–
Diamine + TPPO	31.3	–
DGEBA + TPP_a	−14.6	–
DGEBA + TPPO	30.8	–
DGEBA + TPP_i	126.0, −14.6 (5 h)	72
DGEBA + TPP_i + T403	126.0, 128.6 (4 h), 132.0, −14.6	4
DGEBA + TPP_i + BDMA + T403 – 1 h	126.1, 129.3, 128.6, −14.6	2
DGEBA + TPP_i + BDMA + T403 – 2 h	126.1, 128.6, −14.6	2
DGEBA + T403	–	5

Fig. 7 shows the FTIR spectrum of uncured epoxy resin (DGEBA), triphenyl phosphite (TPP_i) and the accelerated reaction mixture (DGEBA + TPP_i + T403 + BDMA). The uncured EP displays a prominent broad hydroxyl peak at 3500 cm^{-1}, which disappears after 2 h when TPP_i is present and at the same time there is no change in the epoxy group at 912 cm^{-1}. The new band at 692 cm^{-1} corresponds to the P—C and the peak at 1486 cm^{-1} and 1592 cm^{-1} are assigned to Ph-P, both deriving from the phosphorus flame retardants, indicates that TPP_i reacts with the hydroxyl group of the epoxy resin.

Phosphorus nuclear magnetic resonance spectroscopy easily detects the interaction of phosphorus flame retardants with diamine (for PU) and DGEBA. Table 2 shows the characteristic chemical shift (δ) of different oxidation states of phosphorus flame retardants and the phosphorus FR mixed with diamine and epoxy resin. All three phosphorus flame retardants show a single sharp peak in addition to the reference peak [18]. No additional peaks are observed from the mixture containing diamine/DGEBA with phosphorus flame retardants, except in the case of epoxy with TPP_i, where the additional resonance peaks at 128.6, 129.3 and 132 ppm are attributed to the formation of alkyl phenyl phosphites[13]. At the same time, a very small peak, due to TPP_a at −14.6 ppm was observed in mixture

containing TPP_i and both diamine and epoxy resin, which indicates that both trans-esterification and oxidation of TPP_i (for PU) occur simultaneously during curing of epoxy resin.

3.3. TG/FTIR analysis

In general, thermogravimetric analysis (TG) coupled with Fourier transform infrared spectroscopy (FTIR) is used to analyze the gaseous products during a thermal degradation process and also probe the degradation mechanism of polymeric materials [19]. All three phosphorus flame retardants were subjected to TG–FTIR analysis under inert condition. Phenol is the main decomposition product formed for all three materials, but at varying temperature and time. For instance, the maximum degradation of TPP_i takes place rapidly (13 min) at lower temperature compared to TPP_a (14 min) and TPPO (16 min).

Fig. 8 shows the 3D patterns of neat (a) and flame retarded PU (c and d) filled with phosphorus compounds in different oxidation states. Both neat and flame retarded PU samples show a two-step degradation with different evolution time of the decomposition products. As shown in Fig. 8a, the first maximum degradation of PU takes place
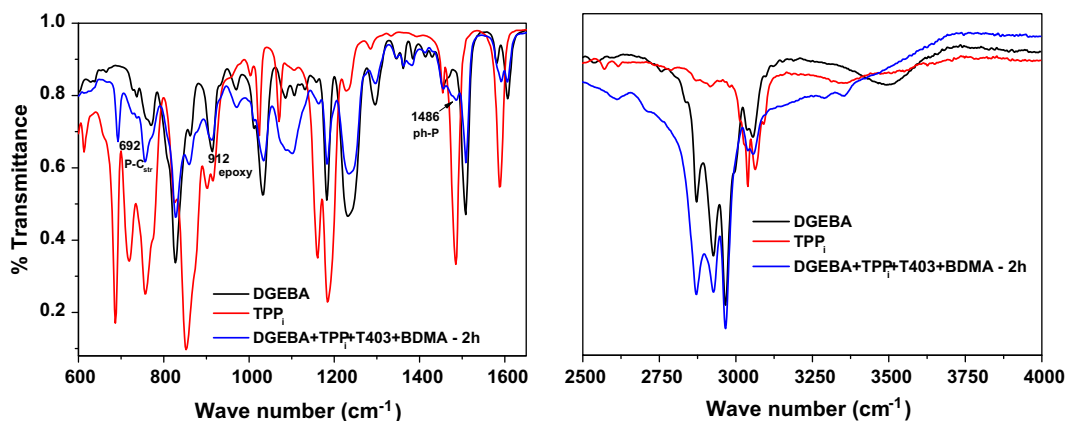
Fig. 7. FTIR of reaction between triphenyl phosphite with hydroxyl group of epoxy.
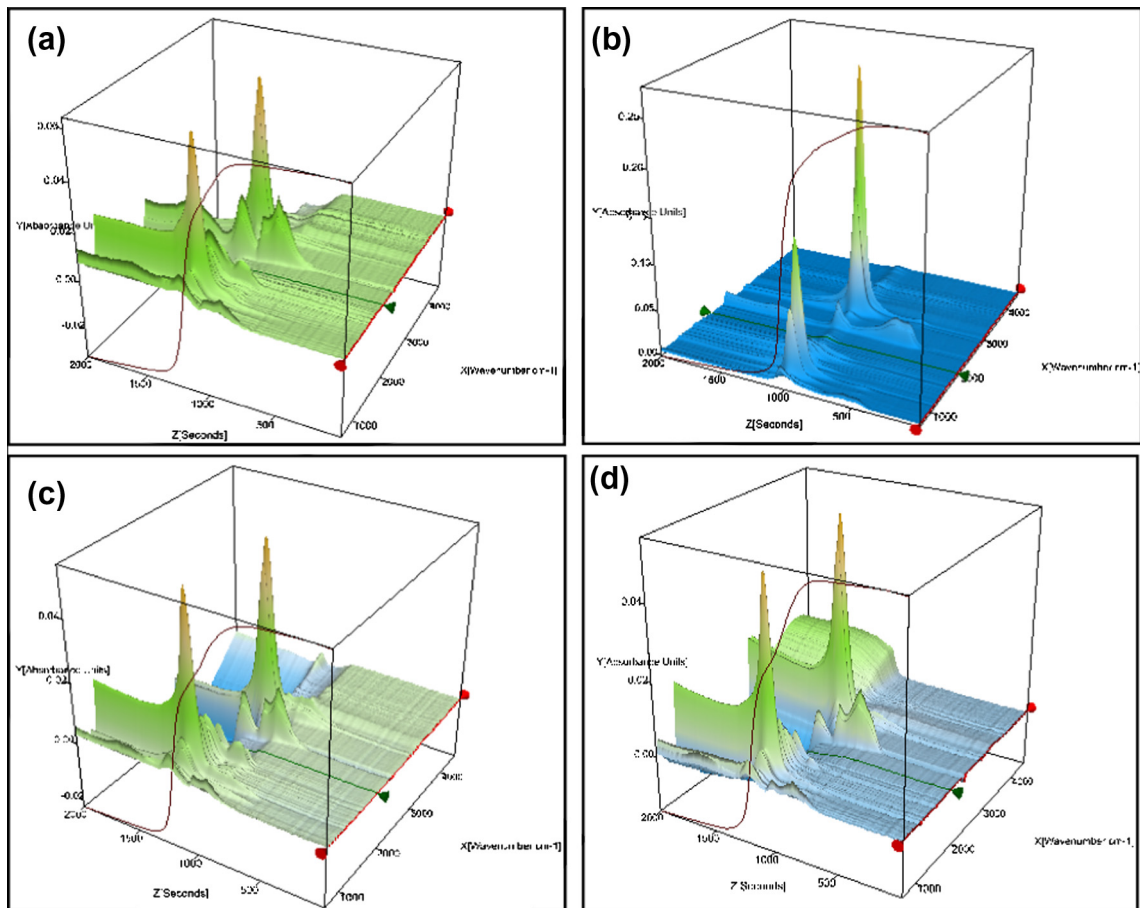
Fig. 8. 3D images of degradation of polyurea filled with phosphorus compounds; (a) PU; (b) PU + TPP$_i$; (c) PU + TPP$_a$; (d) PU + TPPO.

at 322 °C (15 min) and the second maximum degradation occurs at 419 °C (20 min). The first (250 °C) and second maximum degradation temperature (364 °C) and their corresponding times (10 and 17 min) decrease with addition of TPP$_i$ compared to TPP$_a$ and TPPO, which are almost identical with the neat sample.

The decomposition products of PU are identified unambiguously by matching the FTIR peaks with standards using the OMNIC software library search and the characteristic strong FTIR signals. The first step degradation products of PU include isocyanate, hydrocarbons (diamine components), CO_2, and CO and while in the second step, one finds
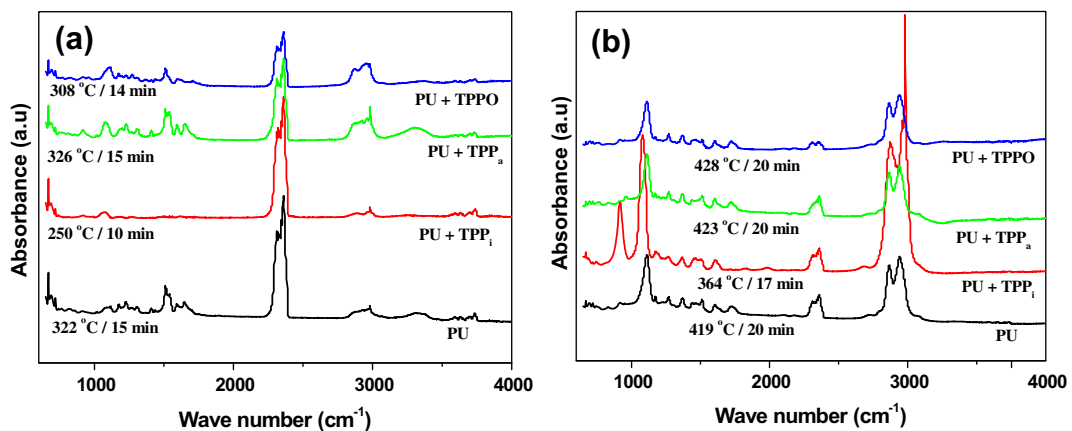
Fig. 9. FTIR of the decomposition of PU and flame retarded PU at first (a) and second (b) degradation maximum rate of weight loss.

propyl and butyl ether, CO_2, and CO; the FTIR spectra are shown in Fig. 9. In the first step, peaks due to urea groups (1511, 1592, 1644 cm^{-1}), isocyanates (2273 cm^{-1}), ether (1177, 1117 cm^{-1}), C—H aliphatic (2981, 2868 cm^{-1}) (derived from diamine fragments), H_2O (3733, 3705, 1305 cm^{-1}) and CO_2 (2359 cm^{-1}) can be found. In the second step, the absorbance of ether (1262, 1174, 1111 cm^{-1}), aromatic (1604, 1510 cm^{-1}), C=O (1725 cm^{-1}), aliphatic hydrocarbons (2942, 2866 cm^{-1}), CO_2 (2359 cm^{-1}), and CO (2177 cm^{-1}) are identified. The breaking of the urea linkage takes place in the first stage and then hydrocarbon scission occurs in the second stage during decomposition of PU.

There is little change in the degradation mechanism of PU upon the addition of the phosphorus flame retardants. In the second stage, the decomposition products of PU differ when TPP_i is added compared to TPP_a and TPPO. For example, tetrahydrofuran (THF) is formed in the second stage of decomposition of TPP_i filled PU. As shown in Fig. 9, the addition of TPP_i reduces the amount of early decomposition products formed in the first stage (a) whereas in the second stage (b), there seems to be a greater amount of phosphates (P—O—C; 918, 1080 cm^{-1}) and hydrocarbons (C—H aliphatic; 2979, 2875 cm^{-1}). In addition, the disappearance of the carbonyl group (1725 cm^{-1}) is observed in the second stage of decomposition of PU filled with TPP_i. Apparently,

TPP_i modifies the degradation products of PU and also promotes the formation of more fuel (hydrocarbons) during pyrolysis. This result corroborated with flame resistance measured by cone calorimetry, as shown in Table 1.
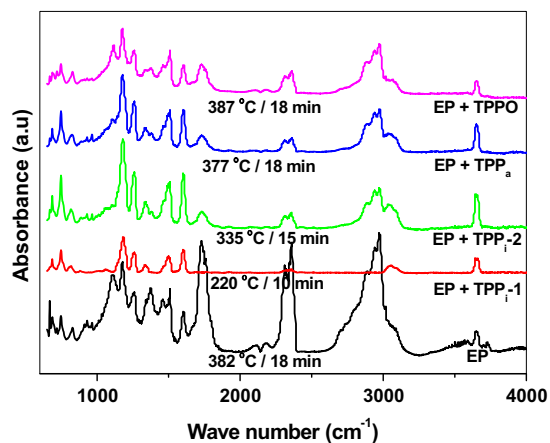
Fig. 11. FTIR of the pyrolysis of EP and flame retarded EP at the maximum rate of weight loss.
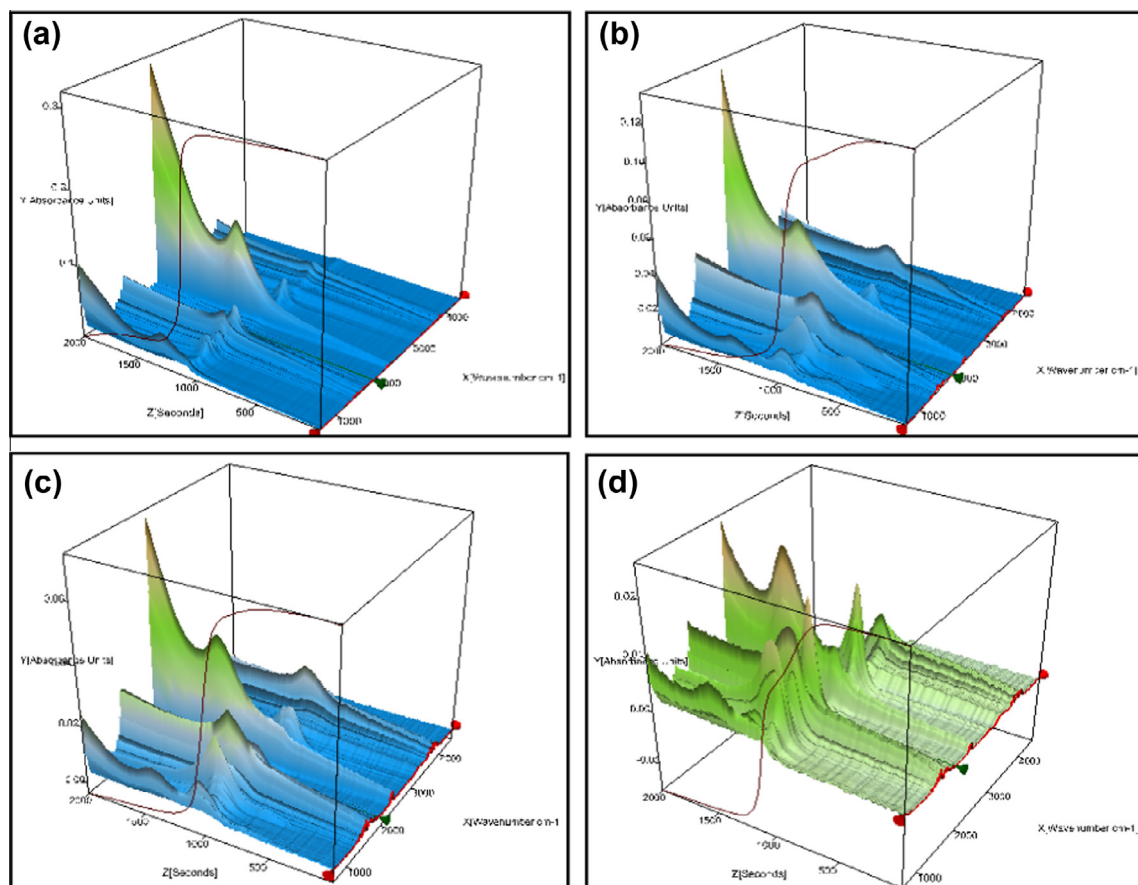
Fig. 10. 3D diagram of degradation of epoxy filled with phosphorus compounds; (a) EP; (b) EP + TPP_i; (c) EP + TPP_a; (d) EP + TPPO.

The 3D profiles of the decomposition of EP and flame re-tarded EP are shown in Fig. 10. The main decomposition products of epoxy resin are acetone, alcohol (bisphenol-A, allyl alcohol, phenol, and amino alcohol), ether, various hydrocarbons, CO_2, CO and H_2O [20]; the analogous FTIR are shown in Fig. 11. The absorbance peaks of acetone (1731 cm^{-1}) phenol/bisphenol-A (3654 cm^{-1}), hydrocar-bons (C—H aliphatic, 2971 cm^{-1}), ether groups (1259, 1177, 1105 cm^{-1}), aromatic (1509 cm^{-1}), CO (2187 cm^{-1}), CO_2 (2358 cm^{-1}) and H_2O (3726, 1373 cm^{-1}) are clearly present. There is no change in degradation products of epoxy with incorporation of phosphorus flame retardants. However, prompt degradation occurs in accordance with the thermal stability of the flame retardants. As shown in

Fig. 10b, the TPP$_i$ filled sample shows an early (10 min) re-lease of degradation products at 220 °C and then the max-imum degradation occurs at 335 °C (15 min). The temperature for the maximum release of the degradation products for neat (382 °C) and TPP$_a$ (377 °C) and TPPO (387 °C) filled EP samples are almost the same.

3.4. XPS analysis

X-ray photoelectron spectroscopy (XPS) is a surface chemical analysis that is used to measure of elemental composition of the surface materials (top 1–10 nm) quan-titatively and also measures the chemical state (valence), chemical bonding environment, empirical formula and

Table 3
XPS analysis of atomic concentration of the phosphorus filled polyurea samples at different temperature.

Sample	Temperature (°C)	Carbon (wt.%)	Oxygen (wt.%)	Phosphorus (wt.%)	P/C (%)	P/O (%)
Polyurea	RT	75.4 ± 0.9	24.2 ± 0.7	0.4 ± 0.4		
	100	76.1 ± 1.1	23.9 ± 1.1	0		
	200	76.0 ± 0.1	23.9 ± 0	0.1 ± 0.1		
	300	84.4 ± 1.5	17.4 ± 1.5	0.1 ± 0		
	400	88.2 ± 0.7	11.6 ± 0.7	0.1 ± 0		
PU + TPP$_i$	RT	73.7 ± 1.0	24.4 ± 0.6	1.9 ± 0.5	2.6	7.7
	100	68.0 ± 2.5	28.3 ± 2.1	3.7 ± 0.5	5.4	13.0
	200	–	–	–	–	–
	300	81.4 ± 2.4	18.3 ± 2.0	0.4 ± 0.4	0.4	2.0
	400	85.5 ± 0.3	14.0 ± 0.6	0.5 ± 0.3	0.6	3.7
PU + TPP$_a$	RT	77.0 ± 0.2	22.0 ± 0.3	1.0 ± 0.1	1.3	4.4
	100	70.4 ± 1.7	27.4 ± 1.3	2.1 ± 0.5	3.0	7.8
	200	75.3 ± 0.6	23.6 ± 0.4	1.1 ± 0.3	1.5	4.9
	300	81.8 ± 0.9	18.0 ± 0.9	0.2 ± 0.1	0.3	1.4
	400	87.3 ± 1.6	12.1 ± 1.6	0.6 ± 0.1	0.6	4.7
PU + TPPO	RT	80.6 ± 0.4	18.8 ± 0.3	0.6 ± 0	0.8	3.3
	100	74.3 ± 0.6	25.0 ± 0.5	0.7 ± 0.2	1.0	2.9
	200	76.5 ± 0.2	22.7 ± 0.1	0.8 ± 0.1	1.0	3.5
	300	79.1 ± 0.5	20.8 ± 0.4	0.1 ± 0.1	0.2	0.7
	400	92.0 ± 3.0	8.0 ± 3.0	0.2 ± 0.1	0.2	2.5

Table 4
XPS analysis of atomic concentration of the different temperature of phosphorus compounds filled epoxy samples.

Sample	Temperature (°C)	Carbon (wt.%)	Oxygen (wt.%)	Phosphorus (wt.%)	P/C (%)	P/O (%)
Epoxy	RT	82.2 ± 0	17.8 ± 0	0		
	100	73.5 ± 0.6	26.2 ± 0.6	0.2 ± 0.1		
	200	72.1 ± 0	27.4 ± 0.2	0.4 ± 0.2		
	300	75.2 ± 0.1	24.4 ± 0.2	0.4 ± 0.1		
	400	71.3 ± 2.0	25.9 ± 1.7	0		
EP + TPP$_i$	RT	79.2 ± 2.7	20.3 ± 2.5	0.5 ± 0.2	0.6	2.5
	100	73.0 ± 0.5	25.7 ± 0.4	1.0 ± 0.2	1.4	4.0
	200	77.4 ± 0.2	21.3 ± 0.4	1.3 ± 0.1	1.7	6.3
	300	86.2 ± 0.5	12.8 ± 0.6	1.0 ± 0	1.1	7.7
	400	75.5 ± 3.5	23.3 ± 3.4	1.1 ± 0.2	1.5	5.0
EP + TPP$_a$	RT	82.3 ± 0.6	17.0 ± 0.5	0.6 ± 0.1	0.8	5.9
	100	75.7 ± 0.6	23.9 ± 0.6	0.5 ± 0	0.6	2.0
	200	75.2 ± 0.4	24.2 ± 0.5	0.6 ± 0.1	0.8	2.4
	300	86.0 ± 0.2	13.0 ± 0.3	1.1 ± 0.1	1.3	8.8
	400	84.0 ± 0.5	14.8 ± 0.5	1.3 ± 0.2	1.6	9.1
EP + TPPO	RT	79.0 ± 0.9	20.6 ± 0.9	0.4 ± 0.1	0.5	1.9
	100	78.9 ± 0.7	20.8 ± 1.1	0.3 ± 0.1	0.4	1.4
	200	77.9 ± 0.8	21.6 ± 0.8	0.6 ± 0	0.7	2.6
	300	78.1 ± 0.6	21.4 ± 0.6	0.5 ± 0.1	0.6	2.2
	400	83.7 ± 0.4	15.8 ± 0.5	0.4 ± 0.1	0.5	2.8

electronic state (oxidation state) of the elements that exists within the materials. The XPS technique is very surface sensitive because only electrons emitted from atoms near the surface escape without losing energy [21–25,18–22]. In this study, the XPS investigations were performed after degradation at various temperatures, 25, 100, 200, 300 and 400 °C, and their particular elemental compositions were measured at three different locations on the sample surface and the average values are reported.

Tables 3 and 4 shows the different elemental (carbon, oxygen and phosphorus) compositions present in the surface of neat and flame retarded PU and EP after degradation at the different temperatures. For neat PU, the amount of carbon at the surface increases with increasing temperature and at the same time oxygen depletion is observed. On the other hand, below 400 °C there is no significant change of composition for neat EP.

Upon incorporation of TPP$_i$, a decreasing amount of phosphorus is present on the surface of PU as the temperature increases but an almost constant amount of phosphorus is present in epoxy. TPP$_i$ volatizes at about 200 °C from PU samples, whereas, due to the trans-esterification reaction between TPP$_i$ and EP, phosphorus builds up in the main chain of the EP and thus the amount of phosphorus is almost constant. Furthermore, because of the plasticizing effect of TPP$_i$, the PU sample becomes liquid at 200 °C. This result is in good agreement with the flame retardant properties of PU and EP measured by cone calorimetry and shown in Table 1. An almost similar amount of phosphorus is present on the surface of PU filled with TPP$_a$, while at high temperature the amount of phosphorus is slightly increased in epoxy. The smaller amount of phosphorus present on the surface of both samples filled with TPPO as a function of different temperature suggests that TPPO acts by vapor phase flame retardant action.

4. Conclusion

The oxidation state of phosphorus-based flame retardants, the thermal stability and possible interactions during burning are considered for effective flame retardancy in both PU and EP. Triphenylphosphite shows significant reduction of the flammability of epoxy resins while triphenylphosphate is more effective for polyurea. A non-conventional intumescent char is formed with addition of triphenylphosphite in epoxy resin, caused by trans-esterification reaction between hydroxyl group and triphenylphosphite. As a consequence of plasticization, the PU matrix showed poor flame resistance with incorporation of triphenylphosphite. The gel time, FTIR, ^{31}P NMR

and XPS analysis confirmed the interaction of epoxy resin with triphenylphosphite.

In this study, attention has been focused on the oxidation state of the phosphorus-containing additive. It must be noted here that reactions that occur are the result of some chemical reactions between the reaction partners. In many cases, this will be a reaction of degradation products. Thus the identity of the reactants and the kinetics of their reactions will have great effect and must be considered. This will be a topic of future investigations.

References

[1] Troitzsch J. International plastics flammability handbook. New York: Hanser; 1990.
[2] Grand AF, Wilkie CA. Fire retardancy of polymeric materials. New York: Marcel Dekker; 2000.
[3] Green J. J Fire Sci 1992;10:470.
[4] Levchik SV, Weil ED. J Fire Sci 2006;24:345.
[5] Wilkie CA, Morgan AB. Fire retardancy of polymeric materials. 2nd ed. New York: CRC; 2010.
[6] Schartel B. Materials 2010;3:4710.
[7] Joseph P, Tretsiakova-McNally S. Polym Adv Technol 2011;22:395.
[8] Braun U, Balabanovich AI, Schartel B, Knoll U, Artner J, Ciesielski M, et al. Polymer 2006;47:8495.
[9] Lorenzetti A, Modesti M, Besco S, Hrelja D, Donadi S. Polym Degrad Stab 2011;96:1455.
[10] Hastie JW. J Res Nat Bur Satnd Sect A Phys Chem 1973;771:773.
[11] Pawlowski KH, Schartel B. POlym Int 2007;56:1404.
[12] Perret B, Pawlowski KH, Schartel BJ. Therm Anal Calorim 2009;97:949.
[13] Awad WH, Wilkie CA. Polymer 2010;51:2277.
[14] Mariappan T, Wilkie CA. PMSE preprints. In: 243rd ACS national meeting – @@ – exposition, San Diego, California; March 25–29, 2012.
[15] Report of the committee on fire safety aspects of polymeric materials, vol. 5. National Academy of Sciences, Washington, DC, 1979.
[16] Barnstorff HD, Ames DP, Chadwick DH. Am Chem Soc Div Paint Plastics Printing Ink Chem. 1959;19(2):178.
[17] Mastrorilli P, Muscio F, Nobile CF, Suranna GP. J Mol Catal A 1999;148:17.
[18] Van Wazer JR, Callis CF, Shoolery JN, Jones RC. Nucl Mag Reson Phosphorus Compd 1956;78:5715.
[19] Wilkie CA. Polym Degrad Stab 1999;66:301.
[20] Guo Y, Bao C, Song L, Yuan B, Hu Y. Ind Eng Chem Res 2011;50:7772.
[21] Mishra AK, Chattopadhyay DK, Sreedhar B, Raju KVSN. Prog Org Coat 2006;55:231.
[22] Wang J, Tu H, Jiang QJ. J Fire Sci 1995;13:261.
[23] Kodolov VI, Shuklin SG, Kuznetsov AP, Makarova LG, Bystrov SG, Demicheva OV, et al. J Appl Polym Sci 2002;85:1477.
[24] Duquesne S, Le Bras M, Jama C, Weil ED, Gengembre L. Polym Degrad Stab 2002;77:203.
[25] Wang J-S, Wang D-Y, Liu Y, Ge X-G, Wang Y-Z. J Appl Polym Sci 2008;108:2644.